Brain Activation During Mental Transformation of Size

Axel Larsen, Claus Bundesen, and Søren Kyllingsbæk
University of Copenhagen

Olaf B. Paulson and Ian Law
The Copenhagen University Hospital

Abstract

■ Visual comparison between different-sized objects with respect to shape can be done by encoding one of the objects as a mental image, transforming the image to the size format of the other object, and then testing for a match (Bundesen, C., & Larsen, A. [1975]. Visual transformation of size. *Journal of Experimental Psychology: Human Perception and Performance, 1,* 214–220). To identify the brain structures implicated in mental transformation of size, we measured the distribution of regional cerebral blood flow (rCBF) by positron emission tomography (PET) in 12 normal subjects who compared random stimulus patterns with respect to shape regardless of variations in size in a one-back match-to-sample paradigm. Each subject was PET-scanned 12 times during repetitive injections of $H_2{}^{15}O$. In one condition (three scans), all stimulus patterns were small. In a second condition (three scans), all stimuli were large. In the third condition (six scans), the stimuli alternated between small and large. Mental transformation of size should occur in the alternating-size condition but not in the fixed-size conditions. As expected, behavioral measures (reaction time [RT], d', β) were nearly the same for the two fixed-size conditions but mean RT was longer and d' smaller in the alternating-size condition. Changes in rCBF specific to mental transformation of size were estimated by contrasting the alternating-size with the fixed-size conditions by use of statistical parametric mapping (SPM96) at a threshold of $p <$ .05 corrected for multiple comparisons. The detected brain structures implicated in mental transformation of size were primarily located in the dorsal pathways, comprising structures in the occipital, parietal, and temporal transition zone (predominantly in the left hemisphere), posterior parietal cortex (bilaterally), area MT/V5 (left), and vermis (bilaterally). Contrasts between the two fixed-size conditions showed significant effects in only the occipital cortex. ■

INTRODUCTION

Our ability to determine if objects are the same in shape, regardless of differences in size, is fundamental in human vision. Size invariance in visual pattern recognition was discussed by Mach (1902) and many later authors as a basic form of stimulus equivalence (e.g., Woodworth & Schlosberg, 1954). Modern treatments of size invariance date back to Pitts and McCulloch (1947), who proposed a neural network model for extraction of size invariant features in the visual cortex. More recently, classification of objects by shape regardless of variations in size has been extensively investigated by reaction time (RT) methods in cognitive psychology.

Bundesen and Larsen (1975) showed their subjects pairs of simultaneously presented random stimulus patterns and asked them to decide as quickly as possible whether the members of a pair were the same in shape regardless of difference in size. Each pair was exposed until the subject responded. The mean time taken to make the comparison was a linearly increasing function of the linear size ratio, s (measured such that s [1), between the stimuli to be compared. Larsen and Bundesen (1978; Experiment 1) obtained essentially the same result when the stimuli to be compared were presented one by one in temporal succession (*successive matching*) rather than side by side at the same time (*simultaneous matching*). The results suggest that the members of a stimulus pair were compared by encoding one of the stimuli as a more or less detailed mental image, transforming the mental image to the size format of the other stimulus, and then testing whether the transformed mental image of the first stimulus matched the visual impression of the second one (for further results and discussion, see Larsen, McIlhagga, & Bundesen, 1999; Larsen & Bundesen, 1998; Cave & Kosslyn, 1989; Ullman, 1989; Jolicoeur & Besner, 1987; Shepard, 1984; Besner, 1983; Kosslyn, 1980; Howard & Kerst, 1978; Besner & Coltheart, 1976).

The results on mental size transformation parallel findings on mental rotation. A classical study by Shepard

and Metzler (1971) showed that the mean time taken to determine that two perspective drawings portrayed objects of the same 3-D shape was a linearly increasing function of the angular difference in orientation between the two objects. Shepard and Metzler concluded that the members of a stimulus pair were compared by mentally rotating one of the depicted objects into the orientation of the other one and then testing for a match. (For further results and discussion, see works collected in Shepard & Cooper, 1982.) RT studies also suggest that combined mental transformations of size and orientation may be used in shape comparisons between objects when the task requires that both differences in size and differences in orientation be ignored (Larsen, 1985; Bundesen, Larsen, & Farrell, 1981; Sekuler & Nash, 1972).

The brain mechanisms involved in mental rotation have been the focus of several recent brain activation studies using functional magnetic resonance imaging (fMRI; McAndrews, Makarec, Crawley, & Mikulis, 1998; Cohen et al., 1996; Tagaris et al., 1996; 1997), positron emission tomography (PET; Alivisatos & Petrides, 1997; Haxby et al., 1993), and recording of event-related potentials (ERP; Pegna et al., 1997; Peronnet & Farah, 1989). All of these studies suggest that the parietal cortices are involved. Three studies (McAndrews et al., 1998; Alivisatos & Petrides, 1997; Cohen et al., 1996) indicate that area MT/V5 might be implicated. Some studies suggest hemispheric specialization (e.g., right hemisphere; Pegna et al., 1997).

To our knowledge, mental transformation of size has not previously been investigated with brain imaging techniques.[1] In the present study we attempted to localize the brain structures involved in mental transformation of size by use of PET $H_2{}^{15}O$ methodology. The methodology puts severe constraints on experimental paradigms because of the short *critical time window* (30–45 sec) during which the radioisotope tissue uptake takes place (Silbersweig et al., 1993). For example, in the successive matching experiment of Larsen and Bundesen (1978; Experiment 1), each trial took about 4 sec. Estimated from the mean RTs, the time consumed by mental size transformation was 55 msec (for size ratio $s = 5$) or less (for $s < 5$) out of the 4 sec. Apparently, by use of the successive matching paradigm employed by Larsen and Bundesen (1978), the number of trials within a critical time window would be limited to about 10, and the total time consumed by mental size transformation would be limited to about half a second per scan.

To enhance the ratio of signal (mental size transformation) to noise in our data, we used a continuous version of the successive matching task: a *one-back match-to-sample task* (cf. Smith & Jonides, 1997). In this paradigm, the subject is presented with a long

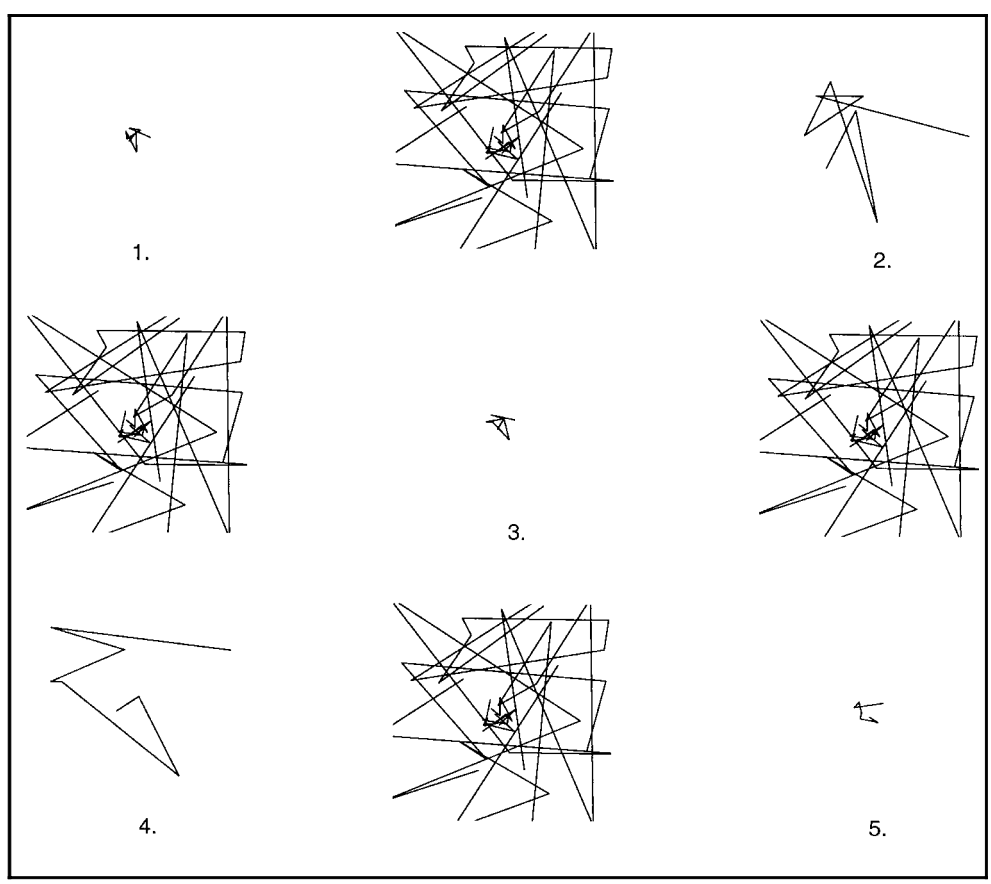

Figure 1. One-back match-to-sample sequence of five stimulus patterns in alternating size (small vs. large). Each stimulus was immediately followed by the postmask, which was constructed by superimposing four large and four small patterns.

sequence of stimuli and asked to compare each stimulus with the immediately preceding one. In our experiment, the stimuli were random patterns (see Figure 1), and the subjects were instructed to press a button each time they detected a pattern that was identical in shape to the immediately preceding one, regardless of any difference in size. Reactions were nonspeeded, and no response should be given when a stimulus differed from the preceding stimulus in shape. The probability that two successive stimuli were the same in shape was .125. With this method, a new stimulus to be compared against the previous one could be presented every 1,300 msec.

The experiment comprised three conditions. In Condition $S_{1,1}$, all stimuli in a sequence were small (Size Format 1). In Condition $S_{6,6}$, all stimuli in a sequence were large (Size Format 6). In Condition $S_{1,6}$, every other stimulus was small (Size Format 1) and every other stimulus was large (Size Format 6). Mental transformation of size should occur in the alternating-size condition ($S_{1,6}$) but not in the fixed-size conditions ($S_{1,1}$ and $S_{6,6}$). By contrasting the brain activation measured in the alternating-size condition with the mean activation measured in the fixed-size conditions, we hoped to find the specific brain structures implicated in mental transformation of size.

Table 1. Speed and Accuracy of Same–Different Classifications with Respect to Shape in Fixed-Size and Alternating-Size Conditions

	Condition			
	$S_{1,1}$	$S_{6,6}$	$S_{1,6}$	ANOVA
RT (ms)	734	728	780	$F(2, 22) = 3.85$, $p < .037$
SD	133	144	115	
False alarm rate	0.03	0.02	0.05	
SD	0.01	0.01	0.02	
Hit rate	0.64	0.66	0.43	
SD	0.18	0.17	0.17	
d'	2.42	2.50	1.48	$F(2, 22) = 69.48$, $p < .001$
SD	0.63	0.63	0.41	
β	6.37	6.82	3.71	$F(2, 22) = 7.02$, $p < .004$
SD	2.34	3.24	0.90	

Mean values across 12 subjects.

RESULTS AND DISCUSSION

Behavioral Data

Table 1 shows summary statistics of RT, hit and false alarm rates, and signal detection measures of discriminability (d') and response bias (β) (see Methods for details). By one-way analyses of variance, the overall effect of condition was significant in both mean RT, d', and β. In each case, however, the difference between the two fixed-size conditions was small, and t tests comparing $S_{1,1}$ and $S_{6,6}$ showed no significant effect on either RT, d', or β: For RT, $t(11) = 0.28$, $p = 0.79$; for d', $t(11) = 0.75$, $p = .47$; for β, $t(11) = 0.41$, $p = .69$. By contrast, we found significant effects on both RT, d', and β by t tests comparing $S_{1,1}$ and $S_{1,6}$: For RT, $t(11) = 2.25$, $p < .05$; for d', $t(11) = 9.59$, $p < .001$; for β, $t(11) = 4.54$, $p < .001$. Similarly, we found significant effects on both RT, d', and β by t tests comparing $S_{6,6}$ and $S_{1,6}$: For RT, $t(11) = 2.56$, $p < .05$; for d', $t(11) = 10.75$, $p < .001$; for β, $t(11) = 3.16$, $p < .01$.

Mean RT was about 50 msec slower and perceptual discriminability d' was about one unit smaller in the alternating-size condition than in the fixed-size conditions. Response bias β was also smaller in the alternating-size than in the fixed-size conditions. Note that β was greater than 1 in all conditions, which indicates a general bias towards *different* rather than *same* decisions. This bias presumably reflects that the a priori probability of a mismatch in shape (.875) was higher than the a priori probability of a match (.125).

The RT findings agree with results obtained in studies of successive matching of random patterns with respect to shape (Larsen et al., 1999; Larsen & Bundesen, 1978). This applies to the finding that, within the range of sizes represented in the experiment, the absolute sizes of the stimuli to be compared had no significant effects on RT, but divergence in size between the stimuli to be compared had a highly systematic effect. It also applies to the strength of the effect due to size divergence: The 50-msec delay obtained in the present experiment with a size ratio of 6 is comparable to the 55-msec delay obtained in the successive matching experiment of Larsen and Bundesen (1978) with a size ratio of 5.

The RT findings suggest the following interpretation of performance in the one-back match-to-sample task. Except for the very first stimulus pattern in a sequence, each new stimulus was compared with a mental image (i.e., a representation in visual short-term memory) of the preceding stimulus and subsequently encoded as a mental image to be compared with the succeeding stimulus. In the alternating-size condition, the comparison of a new stimulus with a mental image of the preceding one was delayed by the time required to transform the mental image of the preceding stimulus to the size format of the new stimulus (about 50 msec). In all other respects, processing was the same in the alternating-size as in the fixed-size conditions. In each condition, we assume, a motor response was initiated as soon as a *same* classification had been made.

The suggested interpretation implies that, although the stimuli were presented at a fixed rate (cf. D'Esposito et al., 1997), the subject was mentally engaged in the one-back match-to-sample task throughout the period in which a scan was done. In the fixed-size conditions, the subject went through a processing cycle of (a) encoding a stimulus as a visual image, (b) retaining the image in visual short-term memory, and (c) comparing the image against the next stimulus, at a rate of once per 1,300 msec. In the alternating-size condition, the subject went through the same cycle at the same rate, except that about 50 msec of the time spent in Phase b was taken up by a mental size transformation of the image held in visual short-term memory.

PET Data

The behavioral data support the assumption that processing was the same in the alternating-size condition as in the fixed-size conditions, except that mental transformation of size occurred in the alternating-size condition but not in the fixed-size conditions. By this assumption, the contrast between the alternating-size condition and the mean of the fixed-size conditions (i.e., $S_{1,6} - 1/2(S_{1,1} + S_{6,6})$) should reveal the cerebral structures that are critical for carrying out mental transformation of size. The contrast is shown in Figures 2 and 3 and Table 2. Most of the regions with increased regional cerebral blood flow (rCBF) seem to belong to the so-called dorsal-visual stream (Milner & Goodale, 1995; Mishkin, Ungerleider, & Macko, 1983), including bilateral posterior parietal cortex and left hemisphere structures in the occipital, parietal, and temporal transition zone and in area MT/V5. In addition, there was reliable evidence of bilateral activation in cerebellum (vermis). No regions showed significant increase in rCBF by the reverse contrast obtained by subtracting the rCBF in the alternating-size condition from the mean rCBF in the fixed-size conditions.

Overall, the pattern of cerebral activity in mental transformation of size shows many similarities with results from brain activation studies of mental rotation. As far as we can ascertain, all studies of mental rotation of visual images implicate superior or posterior parietal cortices (McAndrews et al., 1998; Alivisatos & Petrides, 1997; Pegna et al., 1997; Cohen et al., 1996; Tagaris et al., 1996; 1997; Haxby et al., 1993; Peronnet & Farah, 1989). Some studies (Alivisatos & Petrides, 1997; Tagaris et al., 1997; Cohen et al., 1996) have shown increased rCBF in the inferior parietal lobe. More posterior activation in

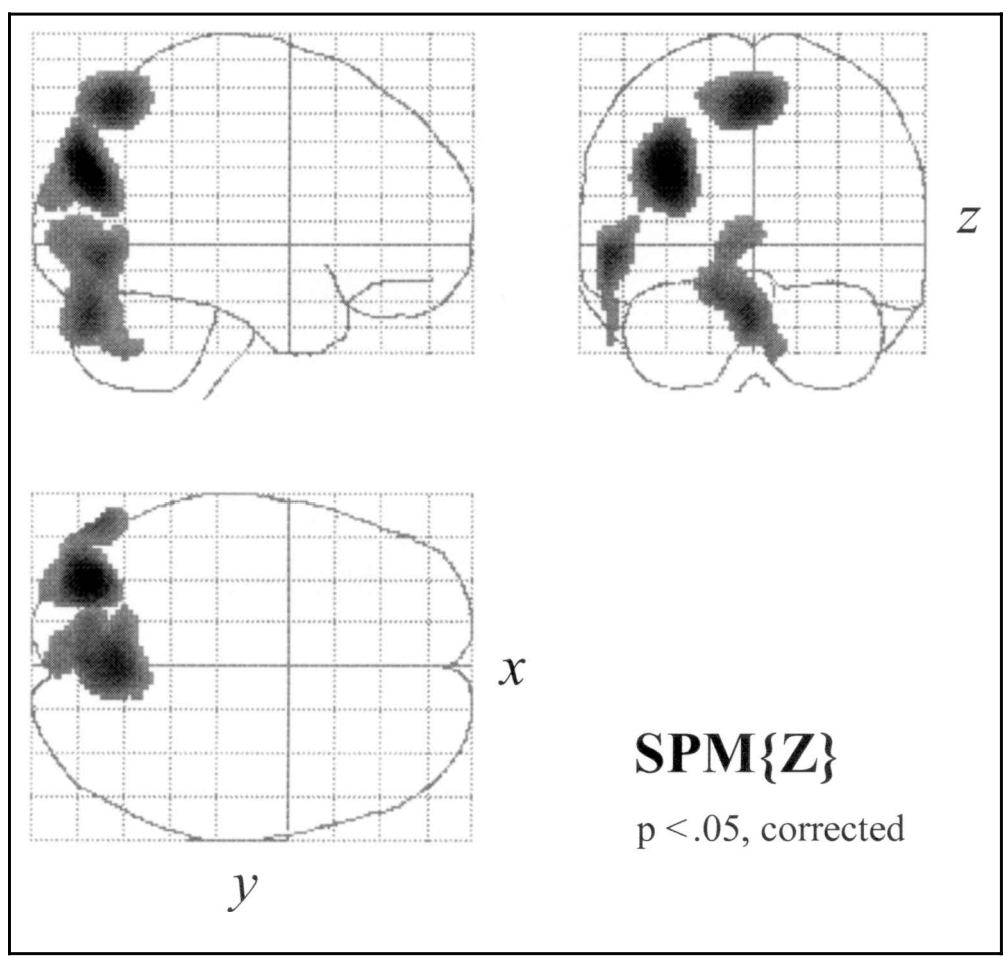

Figure 2. Maximum intensity statistical parametric map (SPM{*Z*}) projections of the contrast between the alternating-size condition and the mean of the fixed-size conditions: $S_{1,6} - 1/2(S_{1,1} + S_{6,6})$.

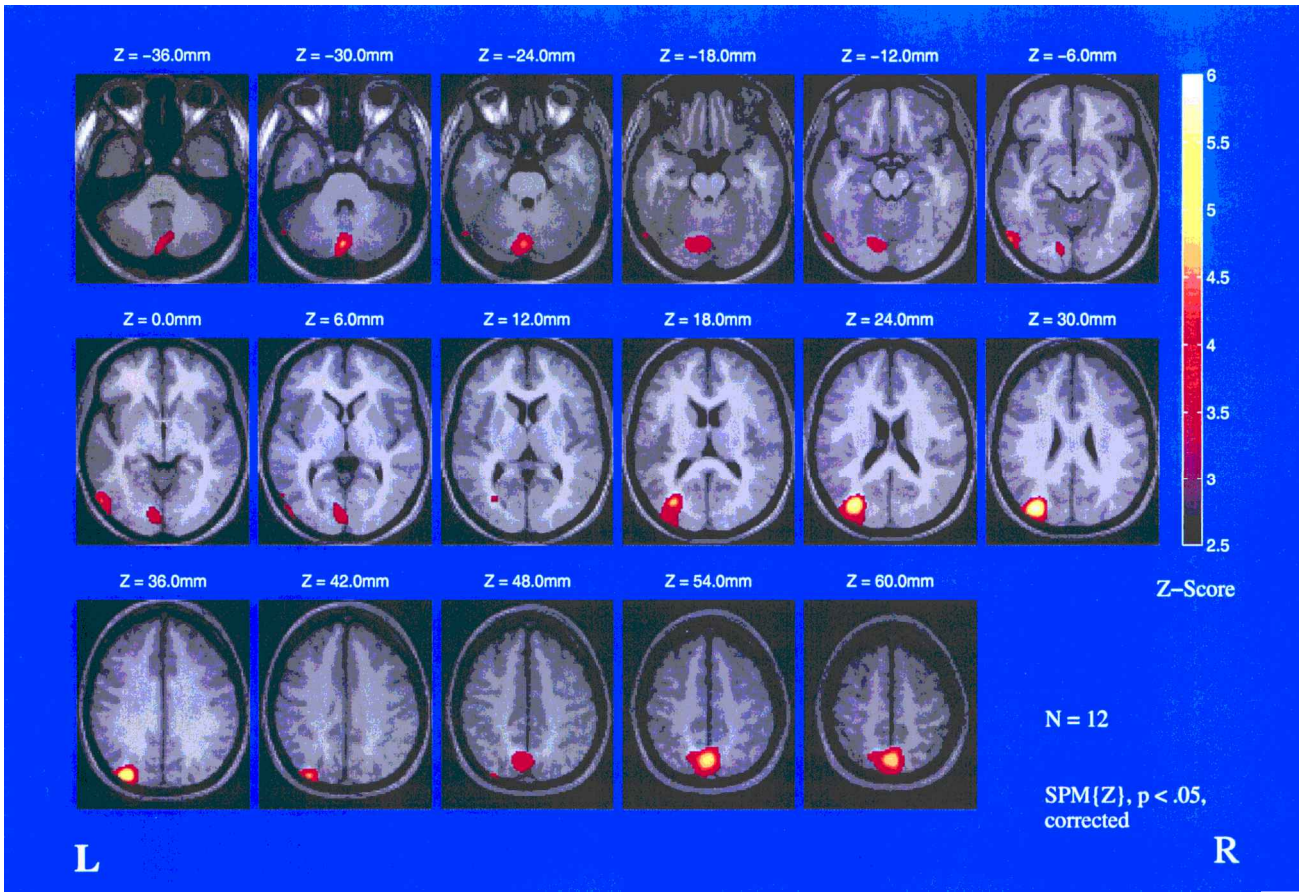

Figure 3. Transverse sections of the statistical parametric map of the contrast $S_{1,6} - 1/2(S_{1,1} + S_{6,6})$ rendered on the average image of the normalized MR brain images of the 12 subjects. Distances above/below the AC–PC plane are given in millimeters. The *Z* scores are mapped to a hot-metal color scale.

the posterior parietal and superior occipital cortices has also been noted (Pegna et al., 1997; Tagaris et al., 1997; Cohen et al., 1996). Alivisatos and Petrides (1997) reported frontal activation (BA 45), and Cohen et al. (1996) found frontal activation (BA 46) in three out of eight subjects. In the present study, eight subjects showed frontal/prefrontal activations ($p < .01$, uncorrected), but the precise location varied between the subjects, and the activations did not add up to a significant focal activation.

We found increased rCBF in area MT/V5 in the mental size transformation condition. The maximum *Z* score in the region was located at $(x, y, z) = (-56, -74, -4)$ (cf. Table 2) corresponding to coordinates $(x, y, z) = (-48, -75, -7)$ in Talairach 88-SPM95 Space. This location seems essentially the same as the locations $(x, y, z) = (45, -76, 3)$ and $(x, y, z) = (42, -69, 0)$ given by Tootell et al. (1995) and Watson et al. (1993), respectively, for MT/V5. As noted above, some brain activation studies of mental rotation have already suggested that area MT/V5 (or areas bordering MT/V5) may be implicated in mental rotation (McAndrews et al., 1998; Alivisatos & Petrides, 1997; Cohen et al., 1996).

MT/V5 is involved in visual perception of motion (cf. Zeki, 1993). Evidence that the same area is implicated in purely mental transformations on objects in space (i.e., in imagined rather than perceived movements) fits in with findings from psychophysical studies comparing mental transformations of size and orientation with visual perception of corresponding apparent movements (Bundesen, Larsen, & Farrell, 1983; Farrell, Larsen, & Bundesen, 1982; Shepard and Judd, 1976). For example, Shepard and Judd (1976) created a perceptual illusion of a rigid object rotating back and forth by showing subjects two different perspective drawings of the same object in sequential alternation. The minimum stimulus-onset asynchrony (SOA) required for seeing apparent rigid rotation was a linearly increasing function of the angular difference in orientation between the two perspective views, so the function was similar to the mental rotation RT function reported by Shepard and Metzler (1971).

Bundesen et al. (1983) created a perceptual illusion of a rigid object in helical or screw-like movement to and fro in depth by presenting two sequentially alternating stimulus patterns that were the same in shape, but

Table 2. Foci of Significant Increase in rCBF During Mental Transformation of Size

Voxels	*Significance*	*Talairach coordinates*					
k	α	*x*	*y*	*z*	*Z score*	Δ*rCBF%*	*Anatomical localization*
1411	.001	0	– 66	56	5.87 (.001)	1.62	Subparietal sulcus, superior-parietal lobule, precuneus, BA 7 (L/R)
1315	.002	– 34	– 78	30	5.16 (.002)	1.85	Left occipital, parietal, temporal junction, middle-occipital gyrus, BA 19
1324	.002	– 2	– 78	– 28	4.62 (.021)	1.33	Vermis (L/R)
398	.041	– 56	– 74	– 4	4.54 (.030)	2.02	Left inferior-temporal gyrus, middle-temporal gyrus (MT/ V5), BA 19

Regions with the designated number of voxels (*k*) are significant as wholes at the indicated levels (α). Within each region, the anatomical location of the voxel with the maximum *Z* score is indexed by the measures established in the MNI-SPM96 implementation of the stereotactic atlas of Talairach and Tournoux (1988). Negative *x*-coordinates indicate left-hemisphere locations. Numbers in parentheses after the maximum *Z* scores are associated levels of significance. Δ rCBF% denotes the mean increase (in percent) of the regional cerebral blood flow (rCBF) in Condition $S_{1,6}$ as compared with the average of Conditions $S_{1,1}$ and $S_{6,6}$. All levels of significance are corrected for multiple comparisons.

differed in size and angular orientation in the fronto-parallel picture plane. The minimum SOA required for the perceptual illusion was a joint function of the size ratio and the angular difference in orientation between the stimuli. The function showed strong similarities to the mean RT functions found in studies of combined mental transformations of size and orientation in shape comparisons between objects (Larsen, 1985; Bundesen et al., 1981). The functional similarities between mental transformations on objects in space and visual perception of objects in motion suggest that some of the same neural circuits that subserve analysis of visual motion may be involved in purely mental transformations on objects.

Two other aspects of our data on effects of mental transformation of size should be considered. First, the significant rCBF increase in vermis in the mental size transformation condition was not anticipated. We are not sure what the finding means. Activation in the vermis may be due to eye movements, but if eye movements for some reason were stronger in the mental transformation condition, we should also have found robust activation in the frontal eye fields (see, e.g., Law, Svarer, Rostrup, & Paulson, 1998). Another possibility touched upon in recent discussions is that cerebellar neurons, in addition to motor programming, directly contributes to perceptual and cognitive processing (see, e.g., Luft, Skalaj, Stefanou, Klose, & Voigt, 1998; Allen, Buxton, Wong, & Courchesne, 1997; Gao et al., 1996; Leiner, Leiner, & Dow, 1995).

Second, in concordance with many neuropsychological studies of imagery (cf. the review in Farah, 1993), but in contrast with some studies of mental rotation (cf. Pegna et al., 1997), the activations we observed during mental transformation of size were stronger in the left hemisphere. Inspection of individual data, however, showed variability in the pattern of lateralization. Several subjects showed roughly symmetric bilateral activations, and a few subjects showed stronger right than left hemisphere activations. We have no explanation for these variations.

Effects of Absolute Size

Cerebral effects of the absolute size of the stimulus patterns were estimated by comparisons between the two fixed-size conditions ($S_{1,1}$ vs. $S_{6,6}$). The results are shown in Figures 4 and 5 and Table 3. Measured by the distribution of rCBF, the large (≈9° of visual angle) stimulus patterns generated more activation than the small (≈1.5°) patterns in most parts of the occipital cortex. This finding is consistent with well-known results concerning the retinotopic organization of early visual areas in human striate cortex and beyond (DeYoe et al., 1996; Sereno et al., 1995; Shipp, Watson, Frackowiak, & Zeki, 1995; also see Zeki et al., 1991).

Two bilaterally symmetric regions in the posterior banks of the fusiform gyri showed significantly greater rCBF for small than for large stimulus patterns (see Figures 4B and 5). The regions extended to the occipital poles, where central fovea seems represented (cf. DeYoe et al., 1996; Fox, Miezin, Allman, Van Essen, & Raichle, 1987). Apparently, the small stimulus patterns were more effective than the large patterns within the central 1.5° of vision, where the small patterns contained six times as much contour (measured by total length) as the large patterns.

CONCLUSION

To localize the brain structures implicated in mental transformation of size, we estimated the regional neural activity by PET in subjects who compared random stimulus patterns with respect to shape regardless of variations in size in a continuous version of the successive matching task: a one-back match-to-sample task. In

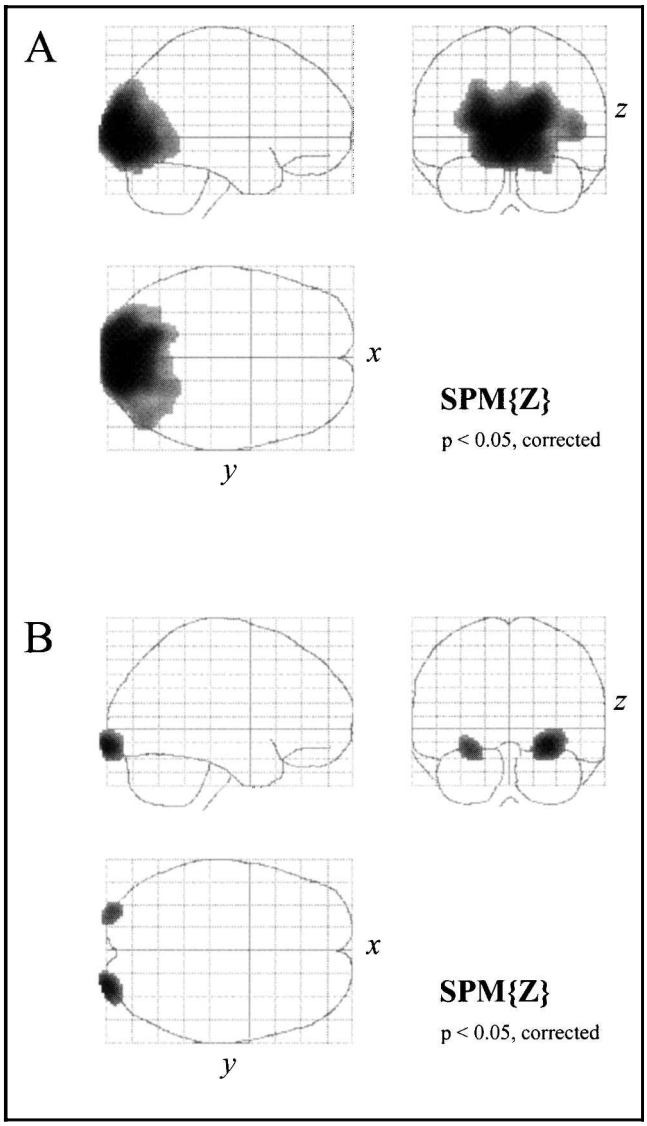

Figure 4. Contrasts between small-stimulus ($S_{1,1}$) and large-stimulus ($S_{6,6}$) conditions. Panel A: Maximum intensity statistical parametric map (SPM{*Z*}) projections of the contrast $S_{6,6} - S_{1,1}$. Panel B: Maximum intensity statistical parametric map (SPM{*Z*}) projections of the contrast $S_{1,1} - S_{6,6}$.

two of the three experimental conditions, the size of the sequentially presented patterns was kept constant, being either small or large. In the third condition, the size of the stimulus patterns alternated between small and large. Mental transformation of size should occur in the alternating-size condition but not in the fixed-size conditions. Behavioral measures (RT, d', β) were nearly the same for the two fixed-size conditions, but mean RT was longer and d' smaller in the alternating-size condition. Changes in brain activation during mental transformation of size were estimated by contrasting the alternating-size condition with the two fixed-size conditions. Regions with increased activation during mental transformation of size were found in the occipital, parietal, and temporal transition zone (predominantly in the left hemisphere), posterior parietal cortex (bilaterally), area MT/V5 (left), and vermis (bilaterally). Contrasts between the two fixed-size conditions showed significant effects in only the occipital cortex.

The activity in MT/V5 during mental transformation of size fits in with psychophysical findings of functional similarities between visual perception of objects in motion and mental transformations on objects in space. The results suggest that some of the same neural circuits that subserve analysis of visual motion are involved in purely mental transformations on objects.

Some of the areas implicated in mental transformation of size may also be implicated in other types of size scaling. A mental image of an external object in a certain size may be defined, in part, as a perceptual readiness for the appearance of that particular object in that particular size. A mental transformation of size is a transformation of a particular mental image. It implies a change in perceptual readiness from a set for perceiving an object with a particular shape in one size format to a set for perceiving an object with that particular shape in another size format. The time course of the process differs from the time course of a change in perceptual readiness from a general set for perception of objects in one size format to a general set for perception of objects in another size format (a *perceptual-scale* transformation; Cave & Kosslyn, 1989; Larsen & Bundesen, 1978). Nevertheless, there may be neural mechanisms (e.g., mechanisms for spatial-frequency tuning) that are shared between mental-image and perceptual-scale transformations. In future studies we plan to investigate the degree of overlap between brain areas implicated in perceptual-scale transformation and areas implicated in mental transformation of size.

METHODS

Subjects

Twelve right-handed subjects (six males, six females, mean age: 24.6 years, range: 22–34) were paid to participate. Informed written consent was obtained according to the Declaration of Helsinki II, and the study was approved by the local ethics committee of Copenhagen (J.nr. (KF) 01-339/94).

Stimuli and Task

Each stimulus was a random white line drawing centered on the black face of a computer-driven cathode-ray tube (CRT). The stimuli were displayed one at a time in a one-back match-to-sample paradigm. To generate the first stimulus in a sequence, 16 random numbers were drawn from a uniform distribution between 0 and 1. The numbers were taken to be the x and y coordinates of 8 points in the unit square, which specified a shape that could be generated by connecting the first with the

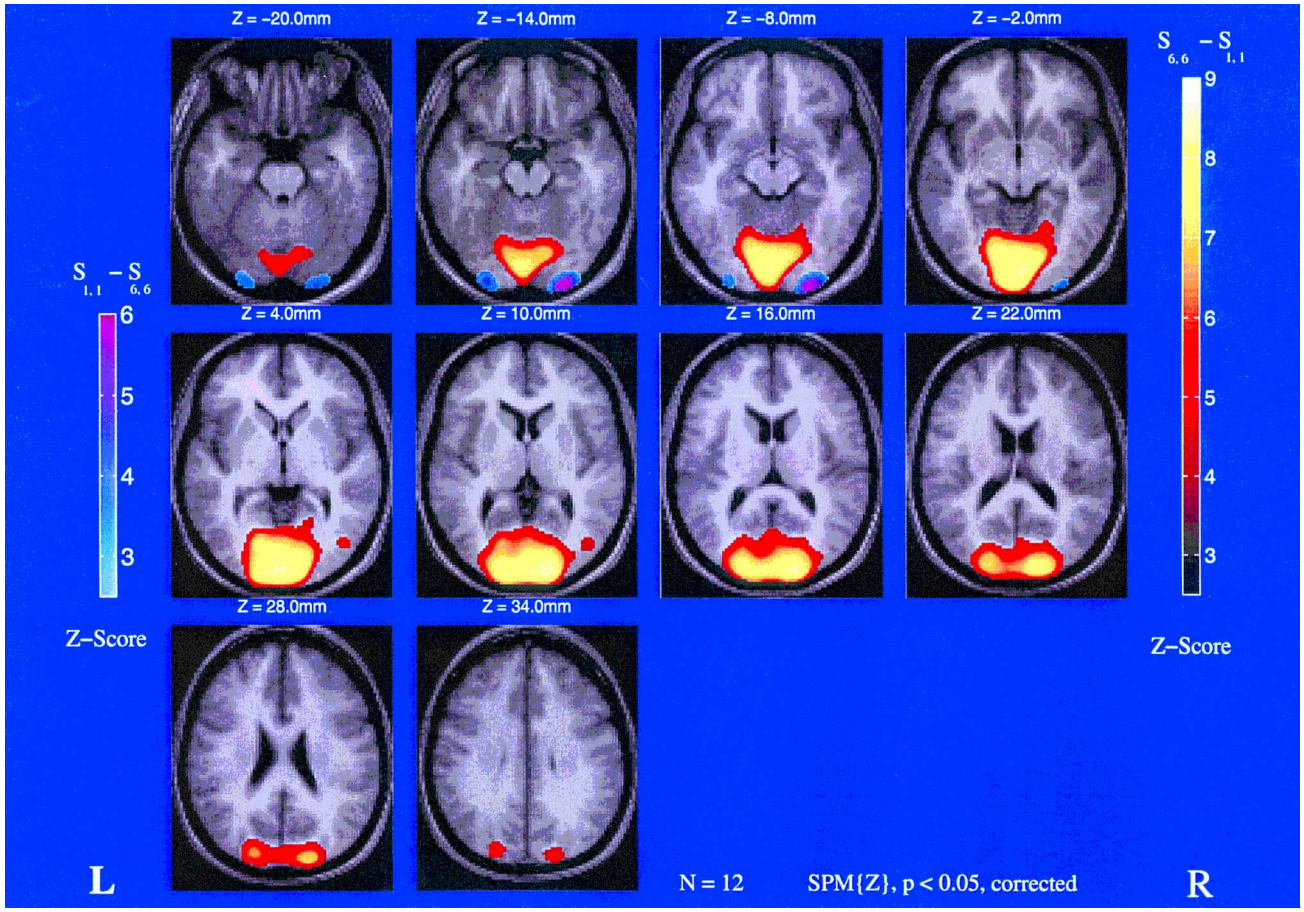

Figure 5. Transverse sections of the statistical parametric map of the contrasts $S_{6,6} - S_{1,1}$ and $S_{1,1} - S_{6,6}$. The contrasts are rendered on the average image of the normalized MR brain images of the 12 subjects. Distances above/below the AC–PC plane are given in millimeters. *Z* scores for the $S_{6,6} - S_{1,1}$ contrast are shown on a hot-metal color scale (right), *Z* scores for the reverse contrast on a cool (cyan–blue–violet) scale (left).

second point, the second with the third point, . . . , and the seventh with the eight point, all connections being made by straight lines. The stimulus could be shown in a small format (Size Format 1) or in a large format (Size Format 6). Small stimuli were generated by mapping the unit square to a 60 × 60 pixels (30 × 30 mm) square on the CRT, whereas large stimuli were generated by mapping the unit square to a 360 × 360 pixels square on the CRT.

The next stimulus in the sequence was identical in shape to the previous one with a probability of .125, but different in shape from the previous one with a probability of .875. In case the stimuli differed in shape, the new stimulus was a random transform of the previous one. The transform was obtained by adding noise components to each of the 16 random numbers (between 0 and 1) that defined the previous stimulus. The noise components were drawn independently from a uniform distribution between – 0.1 and 0.1, but a noise component was changed in sign if the addition of the component otherwise would have moved a stimulus point out of the unit square.

Each stimulus was exposed for 600 msec. When stimulus exposure terminated, a large (360 × 360 pixels) pattern mask was exposed for 33 msec. The mask was created from eight unrelated drawings of possible stimuli: four small ones and four large ones. Both the pattern mask and examples of small and large stimuli are shown in Figure 1. The next stimulus was displayed after a blank interval of 667 msec, so the onset asynchrony between successive stimuli was 1,300 msec.

The subject was instructed to press a button each time he or she detected a stimulus that was identical in shape to the immediately preceding one, regardless of variation in size. Reactions were non-speeded, and no response should be given when a stimulus differed from the preceding one in shape.

Design

The subjects were PET scanned in three conditions. In Condition $S_{1,1}$, all stimuli in a sequence were small (Size Format 1 ≈1.5° of visual angle). In Condition $S_{6,6}$, all stimuli were large (Size Format 6 ≈9° of visual angle). In

Table 3. Foci of Significant Increase in rCBF by Contrasts Between Conditions with Large ($S_{6,6}$) Versus Small ($S_{1,1}$) Stimulus Patterns

Voxels	*Significance*	*Talairach coordinates*					
k	α	*x*	*y*	*z*	*Z score*	Δ*rCBF%*	*Anatomical localization*
$S_{6,6} - S_{1,1}$							
15512	.0001	14	−92	12	8.18 (.0001)	5.11	Occipital lobe, BA 17, 18, and 19, excluding posterior fusiform gyri (L/R)
$S_{1,1} - S_{6,6}$							
504	.001	28	−98	−12	6.21 (.001)	4.43	Right posterior fusiform gyrus, BA 18
254	.002	−29	−96	−14	4.54 (.029)	2.97	Left posterior fusiform gyrus, BA 18

Regions with the designated number of voxels (*k*) are significant as wholes at the indicated levels (α). Within each region, the anatomical location of the voxel with the maximum *Z* score is indexed by the measures established in the MNI-SPM96 implementation of the stereotactic atlas of Talairach and Tournoux (1988). Positive *x*-coordinates indicate right-hemisphere locations. Numbers in parentheses after the maximum *Z* scores are associated levels of significance. ΔrCBF% denotes the mean increase (in percent) of the regional cerebral blood flow (rCBF) in Condition $S_{6,6}$ compared with Condition $S_{1,1}$ ($S_{6,6} - S_{1,1}$) or Condition $S_{1,1}$ compared with Condition $S_{6,6}$ ($S_{1,1} - S_{6,6}$). All levels of significance are corrected for multiple comparisons.

Condition $S_{1,6}$, every other stimulus was small (Size Format 1) and every other stimulus was large (Size Format 6). The subjects were scanned three times in Condition $S_{1,1}$, three times in Condition $S_{6,6}$, and six times in Condition $S_{1,6}$. Each scan was done with a new sequence of 144 stimuli. For each subject, the 12 scans were arranged in an order that was balanced with respect to the three conditions.

Behavioral Measures

Accuracy of performance was analyzed in terms of signal-detection theory (Green & Swets, 1966). A stimulus that required a button press (i.e., a stimulus that was identical in shape to the immediately preceding one) was regarded as a *signal*, and a stimulus that required no button press (i.e., a stimulus that differed in shape from the immediately preceding one) was regarded as *noise*. Let the *hit rate* be the probability that a signal elicited a button press, and let Z_h be the corresponding *Z* score (i.e., the hit rate equals the probability that the unit gaussian variate takes a value that is less than or equal to Z_h). Similarly, let the *false alarm rate* be the probability that a noise stimulus elicited a button press, and let Z_f be the corresponding *Z* score. The discriminability parameter d' of signal-detection theory was computed as $Z_h - Z_f$. The response bias parameter β was computed as $\exp[(Z_f^2 - Z_h^2)/2]$.

PET Procedure

All tasks were initiated approximately 45 sec prior to isotope arrival to the brain, continued during the 90-sec acquisition period, and further continued until the entire sequence of 144 stimuli had been presented. Before the actual experiments began, the subjects practiced outside the scanner in each of the three experimental conditions.

PET scans were obtained with an 18-ring GE-Advance scanner (General Electric Medical Systems, Milwaukee, WI) operating in 3-D acquisition mode, producing 35 image slices with an interslice distance of 4.25 mm. The total axial field of view was 15.2 cm with an approximate in-plane resolution of 5 mm. The technical specifications have been described elsewhere (DeGrado et al., 1994).

For each scan the subject received a slow intravenous bolus injection of 400 MBq (11.4 mCi) of $H_2{}^{15}O$. The isotope was administered via an antecubital intravenous catheter over 30 sec by an automatic injection device. The interscan interval was 10 min. Head movements were limited by head-holders constructed by thermally molded foam. Before the activation sessions a 10-min transmission scan was performed for attenuation correction. Images were reconstructed with a 4.0-mm Hanning filter transaxially and an 8.5-mm Ramp filter axially. The resulting distribution images of time-integrated counts were used as indirect measurements of the regional neural activity (Fox & Mintun, 1989).

MRI Scanning

For accurate anatomical localization of activated foci, structural MRI scanning was performed on every subject with a 1.5-T Vision scanner (Siemens, Erlangen, Germany) using a 3-D MPRAGE sequence (TR/TE/TI = 11/4/100 msec, flip angle 15°). The images were acquired in the sagittal plane with an in-plane resolution of 0.98 mm, and a slice thickness of 1.0 mm. The

number of planes was 170 and the in-plane matrix dimensions were 256 × 256.

Image Analysis

For all subjects the complete brain volume was sampled. Image analysis was performed using Statistical Parametric Mapping software (SPM-96, Wellcome Department of Cognitive Neurology, London, UK; Frackowiak & Friston, 1994). All intra-subject images were aligned on a voxel-by-voxel basis using a 3-D automated 6-parameter rigid body transformation (AIR 3.0; Woods, Cherry, & Mazziotta, 1992), and the anatomical MRI scans were co-registered to the individual averages of the 12 aligned PET scans. The average PET scans and corresponding anatomical MRI scans were subsequently transformed into the standard stereotactic atlas of Talairach and Tournoux (1988) using the PET template defined by the Montreal Neurological Institute (MNI; Friston, Ashburner, et al., 1995). The stereotactically normalized images consisted of 68 planes of 2 × 2 × 2 mm voxels. Before statistical analysis, images were filtered by a 16-mm (FWHM) isotropic gaussian filter to increase the signal-to-noise ratio and to accommodate residual variability in morphological and topographical anatomy that was not accounted for by the stereotactic normalization process (Friston, 1994). Differences in global activity were removed by proportional normalization to a value of 50. Only intracerebral areas that did not change significantly ($p > .05$) between conditions were selected to represent global activity following the iterative approach described by Andersson (1997). The null hypothesis of no regionally specific activation effects of the experimental conditions was tested by comparing conditions on a voxel-by-voxel basis. The resulting set of voxel values constituted a statistical parametric map of the t statistic, SPM$\{t\}$. A transformation of values from the SPM$\{t\}$ into the unit gaussian distribution using a probability integral transform allowed changes to be reported in Z scores (SPM$\{Z\}$). Voxels were considered significant if their Z score exceeded a threshold of $p < .05$ after correction for multiple nonindependent comparisons. This threshold was estimated according to Friston, Frith, Liddle, & Frackowiak (1991) and Friston, Holmes, et al. (1995) using the theory of gaussian fields. The resulting foci were then characterized in terms of peak Z score above this level. To relate our results to findings reported in Talairach-88 SPM95 Space, we used the following transformation (Andreas Meyer-Lindenberg, personal communication) from coordinates in the Talairach-88 MNI SPM96 Space to coordinates in the Talairach-88 SPM95 Space:

$$x_{spm95} = 0.88x_{spm96} + 0.8$$

$$y_{spm95} = 0.97y_{spm96} - 3.32$$

$$z_{spm95} = 0.05y_{fspm96} + 0.88z_{spm96} - 0.44$$

Acknowledgments

This work was supported by a grant from the Danish Research Councils. The staff at the PET Center of the Copenhagen University Hospital, Rigshospitalet, are acknowledged for their help and participation. Furthermore, the John and Birthe Meyer Foundation is gratefully acknowledged for the donation of the Cyclotron and PET scanner.

Reprint requests should be sent to A. Larsen, Center for Visual Cognition, Department of Psychology, University of Copenhagen, Njalsgade 90, DK-2300 Copenhagen S, Denmark.

Note

1. Effects of the size of singly presented shapes have been investigated by single-unit recordings in monkeys. For example, Tanaka, Saito, Fukada, & Moriya (1991) found many cells in anterior inferotemporal cortex that responded selectively to particular shapes (*elaborate* cells). Some of the cells showed a high degree of tolerance to size changes of the stimulus (size invariance). Recognition of objects that are transformed in size have also been studied in monkeys with brain lesions. Weiskrantz and Saunders (1984) found impairments of recognition of familiar objects in unfamiliar sizes in monkeys with inferotemporal or prestriate lesions, but no deficits in animals with lesions of the parietal lobe. However, the bearing of these findings on the location of brain mechanisms involved in transformation of mental images is questionable. Larsen and Bundesen (1978, 1998) argued that normally size invariance in recognition of singly presented, familiar objects is achieved without use of mental images.

REFERENCES

Allen, G., Buxton, R. B., Wong, E. C., & Courchesne, E. (1997). Attentional activation of the cerebellum independent of motor involvement. *Science, 275,* 1940–1943.

Alivisatos, B., & Petrides, M. (1997). Functional activation of the human brain during mental rotation. *Neuropsychologia, 35,* 111–118.

Andersson, J. L. (1997). How to estimate global activity independent of changes in local activity. *Neuroimage, 6,* 237–244.

Besner, D. (1983). Visual pattern recognition: Size preprocessing re-examined. *Quarterly Journal of Experimental Psychology, 35A,* 209–216.

Besner, D., & Coltheart, M. (1976). Mental size scaling examined. *Memory and Cognition, 4,* 525–531.

Bundesen, C., & Larsen, A. (1975). Visual transformation of size. *Journal of Experimental Psychology: Human Perception and Performance, 1,* 214–220.

Bundesen, C., Larsen, A., & Farrell, J. E. (1981). Mental transformations of size and orientation. In J. Long & A. Baddeley (Eds.), *Attention and performance* (pp. 279–294). Hillsdale, NJ: Erlbaum.

Bundesen, C., Larsen, A., & Farrell, J. E. (1983). Visual apparent movement: Transformations of size and orientation. *Perception, 12,* 549–558.

Cave, K. R., & Kosslyn, S. M. (1989). Varieties of size-specific visual selection. *Journal of Experimental Psychology: General, 118,* 148–164.

Cohen, M. S., Kosslyn, S. M., Breiter, H. C., DiGirolamo, G. J., Thompson, W. L., Anderson, A. K., Bookheimer, S. Y., Rosen, B. J., & Belliveau, J. (1996). Changes in cortical activity during mental rotation: A mapping study using functional MRI. *Brain, 119,* 89–100.

DeGrado, T. R., Turkington, T. G., Williams, J. J., Stearns, C. W., Hoffman, J. M., Coleman, R. E. (1994). Performance characteristics of a whole-body PET scanner. *Journal of Nuclear Medicine, 35,* 1398–1406.

D'Esposito, M., Zarahn, E., Aguirre, G. K., Shin, R. K., Auerbach, P., & Detre, J. A. (1997). The effect of pacing of experimental stimuli on observed functional MRI activity. *Neuroimage, 6,* 113–121.

DeYoe, E. A., Carman, G. J., Bandettini, P., Glickman, S., Wieser, J., Cox, R., Miller, D., & Neitz, J. (1996). Mapping striate and extrastriate visual areas in human cerebral cortex. *Proceedings of the National Academy of Sciences, U.S.A., 93,* 2382–2386.

Farah, M. (1993). The neuropsychology of mental imagery. In B. Gulyás, D. Ottoson, & P. E. Roland (Eds.), *Functional organization of the human visual cortex* (pp. 233–240). Oxford: Pergamon.

Farrell, J. E., Larsen, A., & Bundesen, C. (1982). Velocity constraints on apparent rotational movement. *Perception, 11,* 541–546.

Fox, P. T., Miezin, F. M., Allman, J. M., Van Essen, D. C., & Raichle, M. E. (1987). Retinotopic organization of human visual cortex mapped with positron-emission tomography. *Journal of Neuroscience, 7,* 913–922.

Fox, P. T., & Mintun, M. A. (1989). Noninvasive functional brain mapping by change-distribution analysis of averaged PET images of $H_2{}^{15}O$ tissue activity. *Journal of Nuclear Medicine, 30,* 141–149.

Frackowiak, R. S., & Friston, K. J. (1994). Functional neuroanatomy of the human brain: Positron emission tomography: A new neuroanatomical technique. *Journal of Anatomy, 184,* 211–225.

Friston, K. J. (1994). Statistical parametric mapping. In R. Thatcher, M. Hallet, T. Zeffiro, J. E. Roy, & M. Huerta (Eds.), *Functional neuroimaging: Technical foundations* (pp. 79–94). San Diego: Academic Press.

Friston, K. J., Ashburner, J., Frith, C. D., Poline, J., Heather, J. D., & Frackowiak, R. (1995a). Spatial registration and normalization of images. *Human Brain Mapping, 2,* 165–189.

Friston, K. J., Frith, C. D., Liddle, P. F., & Frackowiak, R. S. (1991). Comparing functional (PET) images: The assessment of significant change. *Journal of Cerebral Blood Flow and Metabolism, 11,* 690–699.

Friston, K. J., Holmes, A. P., Worsley, K. J., Poline, J., Frith, C. D., & Frackowiak, R. (1995b). Statistical parametric maps in functional imaging: A general linear approach. *Human Brain Mapping, 2,* 189–210.

Gao, J.-H., Parsons, L. M., Bower, J., Xiong, J., Li, J., & Fox, P. T. (1996). Cerebellum implicated in sensory acquisition and discrimination rather than motor control. *Science, 272,* 545–547.

Green, D. M., & Swets, J. A. (1966). *Signal detection theory and psychophysics*. New York: Wiley.

Haxby, J. V., Grady, C. L., Horwitz, B., Salerno, J., Ungerleider, L. G., Mishkin, M., Shapiro, M. B., & Rapaport, S. (1993). Dissociation of object and spatial visual processing pathways in human extrastriate cortex. In B. Gulyás, D. Ottoson & P. E. Roland (Eds.), *Functional organization of the human visual cortex* (pp. 329–340). Oxford: Pergamon Press.

Howard, J. H., Jr., & Kerst, S. M. (1978). Directional effects of size change on the comparisons of visual shapes. *American Journal of Psychology, 91,* 491–499.

Jolicoeur, P., & Besner, D. (1987). Additivity and interaction between size ratio and response category in the comparison of size-discrepant shapes. *Journal of Experimental Psychology: Human Perception and Performance, 13,* 478–487.

Kosslyn, S. M. (1980). *Image and mind.* Cambridge: Harvard University Press.

Larsen, A. (1985). Pattern matching: Effects of size ratio, angular difference in orientation, and familiarity. *Perception and Psychophysics, 38,* 63–68.

Larsen, A., & Bundesen, C. (1978). Size scaling in visual pattern recognition. *Journal of Experimental Psychology: Human Perception and Performance, 4,* 1–20.

Larsen, A., & Bundesen, C. (1998). Effects of spatial separation in visual pattern matching: Evidence on the role of mental translation. *Journal of Experimental Psychology: Human Perception and Performance, 24,* 719–731.

Larsen, A., McIlhagga, W., & Bundesen, C. (1999). Visual pattern matching: Effects of size ratio, complexity, and similarity in simultaneous and successive matching. *Psychological Research*, 62, 280–288.

Law, I., Svarer, C., Rostrup, E., & Paulson, O. B. (1998). Parieto-occipital cortex activation during self generated eye movements in the dark. *Brain, 121,* 2189–2200.

Leiner, H. C., Leiner, A. L., & Dow, R. S. (1995). The underestimated cerebellum. *Human Brain Mapping, 2,* 244–254.

Luft, A. R., Skalej, M., Stefanou, A., Klose, U., & Voigt, K. (1998). Comparing motion- and imagery-related activation in the cerebellum: A functional MRI study. *Human Brain Mapping, 6,* 105–113.

Mach, E. (1902). *Die Analyse der Empfindungen und das Verhältniss des Physischen zum Psychischen* [The analysis of sensations and the relation of the physical to the psychical] (3rd ed.). Jena, Germany: Gustav Fischer.

McAndrews, M. P., Makarec, K., Crawley, A. P., & Mikulis, D. J. (1998). Functional MRI of 3-D mental rotation. A clinical case study. *Neuroimage, 7,* S65.

Milner, D. A., & Goodale, M. A. (1995). *The visual brain in action*. Oxford: Oxford University Press.

Mishkin, M., Ungerleider, L. G., & Macko, K. A. (1983). Object vision and spatial vision: Two cortical pathways. *Trends in Neuroscience, 6,* 414–417.

Pegna, A. J., Khateb, A., Spinelli, L., Seeck, M., Landis, T., & Michel, C. M. (1997). Unraveling cerebral dynamics of mental imagery. *Human Brain Mapping, 5,* 410–421.

Peronnet, F., & Farah, M. (1989). Mental rotation: An event related potential study with a validated mental rotation task. *Brain and Cognition, 9,* 279–288.

Pitts, W., & McCulloch, W. S. (1947). How we know universals. *Bulletin of Mathematical Biophysics, 9,* 127–147.

Sereno, M. I., Dale, A. M., Reppas, J. B., Kwong, K. K., Belliveau, J. W., Brady, T. J., Rosen, B. R., & Tootell, R. B. H. (1995). Borders of multiple visual areas in humans revealed by functional magnetic resonance imaging. *Science, 268,* 889–893.

Sekuler, R., & Nash, D. (1972). Speed of size scaling in human vision. *Psychonomic Science, 27,* 93–94.

Shepard, R. N. (1984). Ecological constraints on internal representation: Resonant kinematics of perceiving, imagining, thinking, and dreaming. *Psychological Review, 91,* 417–447.

Shepard, R. N., & Cooper, L. A. (1982). *Mental images and their transformations*. Cambridge: MIT Press.

Shepard, R. N., & Judd, S. A. (1976). Perceptual illusion of rotation of three-dimensional objects. *Science, 191,* 952–954.

Shepard, R. N., & Metzler, J. (1971). Mental rotation of three-dimensional objects. *Science, 171,* 701–703.

Shipp, S., Watson, J. D. G., Frackowiak, R. S. J., & Zeki, S. (1995). Retinotopic maps in human prestriate visual cortex: The demarcation of areas V2 and V3. *Neuroimage, 2,* 125–132.

Silbersweig, S. D. A., Stern, E., Frith, C. D., Cahill, C., Schnorr, L., Grootoonk, S., Spinks, T., Clark, J., Frackowiak, R., &

Jones, T. (1993). Detection of thirty-second cognitive activations in single subjects with positron emission tomography: A new low-dose $H_2{}^{15}O$ regional cerebral blood flow three-dimensional imaging technique. *Journal of Cerebral Blood Flow and Metabolism, 13,* 617–629.

Smith, E. E., & Jonides, J. (1997). Working memory: A view from neuroimaging. *Cognitive Psychology, 33,* 5–42.

Tagaris, G. A., Kim, S., Strupp, J. P., Andersen, P., Ugurbil, K., & Georgopoulos, A. (1996). Quantitative relations between parietal activation and performance in mental rotation. *NeuroReport, 7,* 773–776.

Tagaris, G. A., Kim, S., Strupp, J. P., Andersen, P., Ugurbil, K., & Georgopoulos, A. (1997). Mental rotation studied by functional magnetic resonance imaging at high field (4 Tesla): Performance and cortical activation. *Journal of Cognitive Neuroscience, 9,* 119–132.

Talairach, J., & Tournoux, P. (1988). *Co-planar stereotaxic atlas of the human brain*. New York: Thieme Medical Publishers.

Tanaka, K., Saito, H.-A., Fukada, Y., & Moriya, M. (1991). Coding visual images of objects in the inferotemporal cortex of the macaque monkey. *Journal of Neurophysiology, 66,* 170–189.

Tootell, R. B. H., Reppas, J. B., Kwong, K. K., Malach, R., Born, R. T., Brady, T. J., Rosen, B. R., & Belliveau, J. W. (1995). Functional analysis of human MT and related visual cortical areas using magnetic resonance imaging. *Journal of Neuroscience, 15,* 3215–3230.

Ullman, S. (1989). Aligning pictorial descriptions: An approach to object recognition. *Cognition, 32,* 193–254.

Watson, J. D. G., Myers, R., Frackowiak, R. S. J., Hajnal, J. V., Woods, R. P., Mazziotta, J. C., Shipp, S., & Zeki, S. (1993). Area V5 of the human brain: Evidence from a combined study using positron emission tomography and magnetic resonance imaging. *Cerebral Cortex, 3,* 79–94.

Weiskrantz, L., & Saunders, R. C. (1984). Impairments of visual object transforms in monkeys. *Brain, 107,* 1033–1072.

Woods, R. P., Cherry, S. R., Mazziotta, J. C. (1992). Rapid automated algorithm for aligning and reslicing PET images. *Journal of Computer Assisted Tomography, 16,* 620–633.

Woodworth, R. S., & Schlosberg, H. (1954). *Experimental psychology*. London: Methuen.

Zeki, S. (1993). *A vision of the brain*. Oxford: Blackwell.

Zeki, S., Watson, J. D. G., Lueck, C. J., Friston, K. J., Kennard, C., & Frackowiak, R. S. J. (1991). A direct demonstration of functional specialization in human visual cortex. *Journal of Neuroscience, 11,* 641–649.